

UNCLASSIFIED

AD NUMBER

AD262734

LIMITATION CHANGES

TO:

Approved for public release; distribution is unlimited.

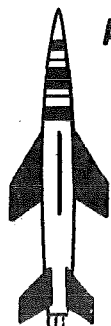
FROM:

Distribution authorized to DoD only;
Administrative/Operational Use; AUG 1961. Other requests shall be referred to Air Force Arnold Engineering Development Center, Arnold AFB, TN.

AUTHORITY

aedc per dtic form 55

THIS PAGE IS UNCLASSIFIED



AEDC-TN-61-87

cy. 4

APR 26 1982

JUL 06 1984

**SOME REYNOLDS NUMBER EFFECTS
ON THE PERFORMANCE OF EJECTORS
WITHOUT INDUCED FLOW**

By

R. C. Bauer and R. C. German
RTF, ARO, Inc.

Phase IV

August 1961

TECHNICAL REPORTS
FILE COPY

**ARNOLD ENGINEERING
DEVELOPMENT CENTER**

AIR FORCE SYSTEMS COMMAND



Additional copies of this report may be obtained from

ASTIA (TISVV)
ARLINGTON HALL STATION
ARLINGTON 12, VIRGINIA

note

Department of Defense contractors must be established for ASTIA services, or have their need-to-know certified by the cognizant military agency of their project or contract.

SOME REYNOLDS NUMBER EFFECTS
ON THE PERFORMANCE OF EJECTORS
WITHOUT INDUCED FLOW

By
R. C. Bauer and R. C. German
RTF, ARO, Inc.

August 1961
AFSC Program Area 750G, Project 6950, Task 69501
ARO Project No. 100928
Contract No. AF 40(600)-800 S/A 24(61-73)

ABSTRACT

The variation of minimum cell pressure ratio with nozzle total pressure level is presented for various ejector configurations having axially symmetric nozzles located on the centerline of cylindrical ducts. Seven nozzles were tested, using unheated air, in combination with two cylindrical ducts of different diameter and of length to diameter ratio equal to or greater than five.

The significant parameter involving nozzle total pressure level was found to be the unit Reynolds number at the nozzle exit times the nozzle throat diameter. For values of this parameter of less than one million, significant variations in the minimum cell pressure ratio occurred. An empirical method, which is usually accurate to within 20 percent of the experimental values, was developed for predicting the variation of minimum cell pressure ratio with nozzle total pressure level for ejectors using 18-deg conical nozzles. Ejectors equipped with contoured nozzles of 0-deg exit angle were found to produce much lower minimum cell pressures for a given nozzle total pressure level than corresponding ejectors equipped with 18-deg conical nozzles although the variation of minimum cell pressure ratio with nozzle total pressure level is similar. Curves are presented which permit the estimation of minimum cell pressure ratio for ejectors using isentropic or other contoured nozzles similar to those used in this investigation.

A similarity parameter is presented which denotes the necessary condition for the equal performance of two geometrically similar ejector systems using different driving fluids.

CONTENTS

	<u>Page</u>
ABSTRACT.	3
NOMENCLATURE.	7
INTRODUCTION	9
APPARATUS	10
PROCEDURE.	11
RESULTS AND DISCUSSION	12
SUMMARY OF RESULTS	18
REFERENCES	19

TABLES

1. Description of Nozzles, Ducting, and Subsonic Diffusers.	21
2. Summary of Test Data.	22

ILLUSTRATIONS

Figure

1. Typical Ejector Configuration	29
2. Typical Nozzle Configurations	30
3. Typical Ejector Starting Phenomena for Constant Nozzle Plenum Total Pressure	31
4. Variation of Minimum Cell Pressure Ratio, p_c/p_{pt} , with Nozzle Plenum Total Pressure Level, p_{pt}	
a. $D_d = 6.09$ in.	32
b. $D_d = 10.19$ in.	33
5. Comparison of Empirical Results with Experimental Data	
a. $D_d = 6.09$ in.	34
b. $D_d = 10.19$ in.	35
c. Data from Ref. 7	36

<u>Figure</u>		<u>Page</u>
6.	Comparison of Empirical Results with Experimental Data	
a.	Data from Configs. 5as ₁ , 5as ₃ , and 5cs ₄ with A_d/A^* as Parameter.	37
b.	Data from Refs. 5 and 7, Configs. 5as ₁ , 5as ₃ , and 5cs ₄ with A_{ne}/A^* as Parameter	38

NOMENCLATURE

A	Cross-sectional area
D	Diameter
K	Correction factor (see Eq. 1)
L_d	Length of cylindrical duct measured from nozzle exit plane
L_s	Length of subsonic diffuser measured from plane of initial divergence
M	Mach number
p	Static pressure
p_{pt}	Nozzle plenum total pressure
R	Reynolds number
T	Static temperature
T_t	Nozzle plenum total temperature
γ	Ratio of specific heats
θ_n	Angle between the nozzle wall and the nozzle centerline at the nozzle exit
θ_s	Angle between the wall and the centerline of the subsonic diffuser

SUBSCRIPTS

c	Ejector cell
d	Duct
ex	Exhaust
ne	Nozzle exit
s	Subsonic diffuser

SUPERScript

$*$	Nozzle throat
-----	---------------

INTRODUCTION

This report presents the results of Phase IV of an ejector research program being conducted in the Rocket Test Facility (RTF) at the Arnold Center, Air Force Systems Command. The subjects covered by the other phases of this research program may be summarized as follows:

Phase I: Effect of nozzle area ratio and diffuser size on the performance of ejectors equipped with 18-deg half angle conical nozzles (Ref. 1)

Phase II: Effect of conical inlets on the performance of ejector systems similar to those studied in Phase I (Ref. 2)

Phase III: Effect of diffuser length on the performance of ejector systems similar to those studied in Phase I (Ref. 3)

The Phase IV study is basically an extension of the Phase I study to include the effect of nozzle total pressure level on the performance of ejectors without induced flow. The data were obtained during the period March 1 through October 19, 1960. Test configurations were selected from those used in the Phase I study, and two new configurations equipped with contoured nozzles having 0-deg exit angles were added.

Other investigators have not defined the effect of nozzle total pressure level on ejector performance, mainly because of facility limitations or interest in other aspects of ejector performance. However, in Ref. 4, base pressure ratio is qualitatively shown to be a strong function of a Reynolds number parameter. The data in this report show a similar variation of minimum cell pressure ratio with a Reynolds number parameter as predicted in Ref. 4.

The Phase IV data are of practical importance in the design of facilities to test at simulated high altitudes proposed space rocket engines having large area ratio nozzles and relatively low combustion chamber pressures. Two available theoretical approaches for predicting minimum cell pressure ratio are presented in Refs. 5 and 6. In Ref. 5 the theory is shown to deviate significantly from experimental data obtained from an ejector system equipped with an isentropic nozzle of area ratio 1.928 and values of A_d/A_{ne} greater than 2.0. The theory presented in Ref. 6 also is shown to deviate

significantly from experimental data obtained from an ejector system equipped with a conical 15-deg half angle nozzle of area ratio 4.235 for values of A_d/A_{ne} greater than 2.0. As a result, to design practical ejector systems, empirical equations are needed embodying all important parameters. Such equations are presented here as derived from the large amount of available experimental data.

APPARATUS

Each of the 13 ejector configurations was equipped with a supersonic nozzle located in a sealed plenum section and a straight cylindrical diffuser. A typical ejector configuration is shown in Fig. 1.

The seven supersonic nozzles used (expansion ratios of 3.627, 5.070, 10.848, 10.962, 23.684, 25, and 100) were each machined in one piece. All nozzles were made of brass, with the exception of the area ratio 10.962 nozzle which was made of steel. Dimensional details of these nozzles are presented in Table 1, and typical nozzle configurations are shown in Fig. 2.

Included in Table 1 are the configuration code designations of the nozzles, the cylindrical ducts, and the subsonic diffusers. A typical ejector configuration designation would be 5cs₄, meaning nozzle configuration 5, duct c, and subsonic diffuser s₄, and the geometry would be

$$A_{ne}/A^* = 23.684$$

$$D_d = 10.19 \text{ in.}$$

$$L_s = 13 \text{ in.}$$

If the configuration did not have a subsonic diffuser, the subsonic diffuser code was dropped from the ejector configuration designation. For the above case, the ejector configuration designation would be 5c.

The following table includes the pressures measured, the pressure ranges, the types of measuring instrument used, and the estimated maximum deviation of the measured pressures.

Pressure Measured	Pressure Range	Measuring Instrument	Estimated Max. Deviation
p_c	0.1 to 50mm HgA	McLeod	
	5 to 50mm HgA	diaphragm-activated dial gage	± 0.20 mm HgA
p_{ex}	7 to 50mm HgA	diaphragm-activated dial gage	± 0.20 mm HgA
	1 to 8 psia	diaphragm-activated dial gage	± 0.03 psia
p_{pt}	1 to 45 psia	diaphragm-activated dial gage	± 0.20 psia
	45 to 150 psia	diaphragm-activated dial gage	± 2 psia
	150 to 380 psia	bourdon tube dial gage	± 5 psia
p_{ne}	1 to 50mm HgA	diaphragm-activated dial gage	± 0.20 mm HgA

The nozzle plenum total temperature ranged from 50 to 306°F and was measured with a copper-constantan thermocouple having an estimated deviation of $\pm 5.0^\circ\text{F}$. The various dimensional deviations are presented in Table 1.

PROCEDURE

Before each test the entire cell was pressure checked with 30-psia air, and all flanges and instrumentation fittings were sprayed with liquid soap to permit detection of any possible leak. In addition, the cell was vacuum checked for leakage.

For each test configuration the nozzle plenum total pressure, p_{pt} , was varied from a minimum to a maximum pressure with the ejector in the "started" condition at all times. A typical ejector operating curve defining the various flow configurations existing for the starting condition is presented in Fig. 3. The minimum cell pressure, p_c , and the nozzle exit static pressure, p_{ne} , were recorded for each nozzle plenum total pressure level. The "starting" pressure ratio, p_{ex}/p_{pt} ,

for each nozzle plenum total pressure level was determined by decreasing the exhaust pressure, p_{ex} , until the cell pressure became independent of the exhaust pressure. The test conditions for each configuration are presented in Table 2.

RESULTS AND DISCUSSION

EXPERIMENTAL RESULTS

A complete tabulation of the experimental results is presented in Table 2. Included in this tabulation are nozzle plenum total pressure, p_{pt} , nozzle plenum total temperature, T_t , minimum cell pressure ratio, p_c/p_{pt} , required starting pressure ratio, p_{ex}/p_{pt} , and nozzle exit static pressure ratio, p_{ne}/p_{pt} . The variation of minimum cell pressure ratio with nozzle plenum total pressure was of primary interest and is graphically presented in Figs. 4a and b. From these data the following ejector characteristics may be noted:

1. The rate of change of minimum cell pressure ratio with nozzle plenum total pressure level became very small as the nozzle plenum total pressure level was increased. This is shown in Figs. 4a and b.
2. For each conical nozzle having a half-cone angle of 18 deg, one nozzle plenum total pressure existed at which the minimum cell pressure ratio was less than the minimum cell pressure ratio corresponding to any other nozzle plenum total pressure level. For ejector configurations equipped with the contoured nozzles having 0-deg exit half angles, experimental data were not obtained at high enough nozzle plenum total pressure level to prove or disprove this fact. These relationships are shown in Figs. 4a and b.
3. The required starting pressure ratio was essentially independent of nozzle plenum total pressure and nozzle exit diameter (Table 2).

The starting pressure ratios presented in Table 2 are, of course, the ratios for the particular configurations tested which had diffuser cylindrical length to diameter ratios, L_d/D_d , greater than or equal to five. As shown in Ref. 3, the starting pressure ratio of an ejector system is a strong function of the ratio L_d/D_d and the nozzle exit half angle, θ_n .

EMPIRICAL ANALYSIS

At the present time, the variation of minimum cell pressure ratio with nozzle plenum total pressure cannot be predicted quantitatively although the shape of this variation has been qualitatively predicted in Ref. 4. Two available theoretical approaches for predicting minimum cell pressure are presented in Refs. 5 and 6. In Ref. 5 the theory is shown to deviate significantly from experimental data obtained from an ejector system equipped with an isentropic nozzle of area ratio 1.928 and values of A_d/A_{ne} greater than 2.0. The theory presented in Ref. 6 also is shown to deviate significantly from experimental data obtained from an ejector system equipped with a conical 15-deg half angle nozzle of area ratio 4.235 for values of A_d/A_{ne} greater than 2.0.

The successful design of practical ejector systems requires a method for estimating ejector performance which includes all the significant variables involved. The inadequacy of present theoretical methods leaves only the empirical approach for solution of this problem.

The simple method of estimating the minimum cell pressure ratio of any ejector system, referred to as one-dimensional theory in Ref. 1, is based on the assumption that the minimum cell pressure ratio equals the ratio of static pressure to total pressure corresponding to the Mach number defined by the ratio of cylindrical diffuser area to nozzle throat area. This method does not include the variables, nozzle exit flow conditions, nozzle exit flow angle, or nozzle plenum total pressure level, but does include the correct trend for variation of specific heat ratio. The simplicity of this method allows its use as the basis of an empirical solution as follows:

An "effective" ratio of cylindrical duct area to nozzle throat area was defined by the following equation

$$(A_d/A^*)_{\text{effective}} = K(A_d/A^*)_{\text{actual}} \quad (1)$$

where

$$K = f[(A_{ne}/A^*), (A_d/A^*), \theta_n, R_{ne}]$$

For ejector configurations equipped with 18-deg conical nozzles, the empirical equation for the correction factor, K , was determined from the experimental data presented in this report by plotting these data as K vs p_{pt} using Eq. (1). From this plot it was found that all data would lie on a single curve when they were plotted as $K(D_d/D_{ne})^{1/4}$ vs $R_{ne}(D^*/D_{ne})$. The shape of the curve resembled that of a displacement-time curve for a "critically" damped spring-mass combination which

suggested the following equation formed with the constants determined by the experimental data

$$K(D_d/D_{ne})^{1/4} = 1 - \frac{3}{2} \ell^{-3.89 R_{ne} (D^*/D_{ne}) (10)^{-6}} + \frac{1}{2} \ell^{-R_{ne} (D^*/D_{ne}) (10)^{-6}} + \frac{1}{2} \ell^{-R_{ne} (D^*/D_{ne}) (10)^{-5}} \quad (2)$$

A comparison of minimum cell pressure ratios calculated using empirical Eq. (2) with the experimental values is presented in Figs. 5a, b, and c. As shown, the empirical equation represented the correct trends of all the variables, excluding nozzle exit flow angle, and was usually accurate to within 20 percent. The data presented in Fig. 5c were obtained from Ref. 7 for ejector configurations equipped with 15-deg conical nozzles. The excellent agreement of Eq. (2) with these data was fortuitous since Eq. (2) does not involve the nozzle exit flow angle.

It can be seen from Figs. 4a and b (compare configuration 5as₁ with 4as₁ and 5cs₂ with 4cs₂) that at a given nozzle total pressure level an ejector equipped with the contoured nozzle produced a much lower minimum cell pressure ratio than an ejector equipped with the 18-deg conical nozzle for the same set of area ratios. The data presently available are insufficient to determine the correct modification of Eq. (2) required to account for the nozzle exit flow conditions.

In general, the nozzle exit flow conditions can be defined by two parameters which determine the shape of the free jet boundary, and these are the nozzle exit wall angle, θ_n , and the Mach number and total pressure distribution functions across the nozzle exit plane. It is interesting to compare the minimum cell pressure ratio calculated using Eq. (2) with experimental values obtained from ejector configurations equipped with isentropic and contoured nozzles. Such a comparison is Fig. 6a which shows that the variation of minimum cell pressure ratio with nozzle total pressure level for an ejector equipped with a contoured nozzle is similar to that represented by Eq. (2) even though the absolute value of this ratio may be different. This may or may not be true for ejectors equipped with isentropic-type nozzles. In Fig. 6b, a similar comparison is made with data obtained from Refs. 5 and 7 and configurations 5as₁ and 5cs₄. The data from Ref. 5 were obtained from ejectors equipped with isentropic-type nozzles; the other data were obtained from ejectors equipped with contoured nozzles. The effect of nozzle plenum total pressure level on the trends shown in Fig. 6b was very small since $R_{ne}(D^*/D_{ne})$ was usually greater than 1.5×10^6 , and Eq. (2) tends to eliminate this variable. The variation of the ratio $(p_c/p_{pt})_{exp}/(p_c/p_{pt})_{cal}$ with the ratio A_d/A_{ne} is of

similar shape for ejectors equipped with either isentropic or contoured nozzles.

Values from Fig. 6b can be used to correct the results from Eq. 2, and thus the performance of other ejector systems equipped with either isentropic or contoured nozzles that are within the limits of these data can be estimated.

Similarity Rule

On the basis of the previous discussion, it is possible to derive the necessary condition to insure the attainment of equal minimum cell pressure ratios for two geometrically similar ejector configurations using entirely different driving fluids. This condition is derived as follows:

Based on the empirical approach, the minimum cell pressure ratio can be expressed as follows from continuity and state equations assuming no phase changes or chemical reactions occur.

$$P_c/P_{Pt} = \frac{(p^*/P_{Pt}) \sqrt{(T_d/T_t)}}{\sqrt{T^*/T_t} M_d K (A_d/A^*)}$$

From energy considerations for isentropic flow

$$p^*/P_{Pt} = \left[1 + \frac{\gamma - 1}{2} \right]^{-\frac{\gamma}{\gamma - 1}} = \left[\frac{2}{\gamma + 1} \right]^{+\frac{\gamma}{\gamma - 1}}$$

and

$$T^*/T_t = \left[1 + \frac{\gamma - 1}{2} \right]^{-1} = \frac{2}{\gamma + 1}$$

$$\therefore \frac{(p^*/P_{Pt})}{\sqrt{T^*/T_t}} = \frac{\left[\frac{2}{\gamma + 1} \right]^{+\frac{\gamma}{\gamma - 1}}}{\left[\frac{2}{\gamma + 1} \right]^{1/2}} = \left[\frac{2}{\gamma + 1} \right]^{\frac{\gamma + 1}{2(\gamma - 1)}}$$

and

$$P_c/P_{Pt} = \left[\frac{2}{\gamma + 1} \right]^{\frac{\gamma + 1}{2(\gamma - 1)}} \frac{\sqrt{(T_d/T_t)}}{M_d K (A_d/A^*)} \quad (3)$$

If subscripts "1" and "2" denote the two geometrically similar ejector configurations, then

$$(p_c/p_{pt})_1 = \frac{\left[\frac{2}{\gamma_1+1}\right]^{\frac{\gamma_1+1}{2(\gamma_1-1)}} \sqrt{(T_d/T_t)_1}}{M_{d1} K_1 (A_d/A^*)_1}$$

and

$$(p_c/p_{pt})_2 = \frac{\left[\frac{2}{\gamma_2+1}\right]^{\frac{\gamma_2+1}{2(\gamma_2-1)}} \sqrt{(T_d/T_t)_2}}{M_{d2} K_2 (A_d/A^*)_2}$$

The requirement for equal minimum cell pressure ratio is

$$(p_c/p_{pt})_1 = (p_c/p_{pt})_2$$

and by geometric similarity

$$\left(\frac{A_d}{A^*}\right)_1 = \left(\frac{A_d}{A^*}\right)_2$$

$$\therefore \frac{\left[\frac{2}{\gamma_1+1}\right]^{\frac{\gamma_1+1}{2(\gamma_1-1)}} \sqrt{(T_d/T_t)_1}}{M_{d1} K_1} = \frac{\left[\frac{2}{\gamma_2+1}\right]^{\frac{\gamma_2+1}{2(\gamma_2-1)}} \sqrt{(T_d/T_t)_2}}{M_{d2} K_2} \quad (4)$$

M_{d1} and M_{d2} are related by the energy equation for isentropic flow as follows

$$\left[1 + \frac{\gamma_1-1}{2} M_{d1}^2\right]^{\frac{\gamma_1}{\gamma_1-1}} = \left[1 + \frac{\gamma_2-1}{2} M_{d2}^2\right]^{\frac{\gamma_2}{\gamma_2-1}}$$

Solving for M_{d1} yields

$$M_{d1} = \left[\frac{1 + \frac{\gamma_2-1}{2} M_{d2}^2 \left(\frac{\gamma_2}{\gamma_1}\right) \left(\frac{\gamma_1-1}{\gamma_2-1}\right) - 1}{\frac{\gamma_1-1}{2}} \right]^{1/2} \quad (5)$$

Also from energy relations

$$(T_d/T_t)_1 = \left[1 + \frac{\gamma_1-1}{2} M_{d1}^2\right]^{-1} \quad (6)$$

When Eq. (5) is substituted into Eq. (6)

$$(T_d/T_t)_1 = \left[1 + \frac{\gamma_2-1}{2} M_{d2}^2\right]^{-1} \left(\frac{\gamma_2}{\gamma_1}\right) \left(\frac{\gamma_1-1}{\gamma_2-1}\right) = (T_d/T_t)_2 \left(\frac{\gamma_2}{\gamma_1}\right) \left(\frac{\gamma_1-1}{\gamma_2-1}\right) \quad (7)$$

Solving Eq. (6) for M_{d1} yields

$$M_{d1} = \left[\frac{1 - (T_d/T_t)_1}{(\gamma_1 - 1)/2 (T_d/T_t)_1} \right]^{1/2} \quad (8)$$

and

$$M_{d2} = \left[\frac{1 - (T_d/T_t)_2}{(\gamma_2 - 1)/2 (T_d/T_t)_2} \right]^{1/2} \quad (9)$$

Then rearranging Eq. (4) yields

$$\frac{K_2}{K_1} = \frac{M_{d1}}{M_{d2}} \frac{\left[\frac{2}{\gamma_2 + 1} \right]^{\frac{\gamma_2 + 1}{2(\gamma_2 - 1)}}}{\left[\frac{2}{\gamma_1 + 1} \right]^{\frac{\gamma_1 + 1}{2(\gamma_1 - 1)}}} \left[\frac{(T_d/T_t)_2}{(T_d/T_t)_1} \right]^{1/2} \quad (10)$$

Substituting Eqs. (7), (8), and (9) into Eq. (10) yields

$$\frac{K_2}{K_1} = \left(\frac{\gamma_2 - 1}{\gamma_1 - 1} \right)^{1/2} \frac{\left[\frac{2}{\gamma_2 + 1} \right]^{\frac{\gamma_2 + 1}{2(\gamma_2 - 1)}}}{\left[\frac{2}{\gamma_1 + 1} \right]^{\frac{\gamma_1 + 1}{2(\gamma_1 - 1)}}} \left[(T_d/T_t)_2 \right]^{\frac{\gamma_2 - \gamma_1}{\gamma_1(\gamma_2 - 1)}} \quad (11)$$

$$\left[\frac{1 - (T_d/T_t)_2}{1 - (T_d/T_t)_1} \right]^{1/2}$$

The equation form of the correction factor K can be obtained for any ejector system by generalizing the empirical Eq. (2) as follows,

$$K = G [A_{ne}/A^*, A_d/A^*, A_d/A_{ne}, \theta_n] R [R_{ne} (D^*/D_{ne})] \quad (12)$$

let

$$G = G [A_{ne}/A^*, A_d/A^*, A_d/A_{ne}, \theta_n]$$

and

$$R = R [R_{ne} (D^*/D_{ne})]$$

Then Eq. (12) can be written

$$K = GR \quad (13)$$

Since the two ejectors being considered are geometrically similar, the ratio K_2/K_1 from Eq. (13) is as follows

$$\frac{K_2}{K_1} = \frac{R_2}{R_1} \quad (14)$$

The substitution of Eq. (14) into Eq. (11) yields

$$\frac{R_2}{R_1} = \left(\frac{\gamma_2 - 1}{\gamma_1 - 1} \right)^{1/2} \frac{\left(\frac{2}{\gamma_2 + 1} \right)^{\frac{\gamma_2 + 1}{2(\gamma_2 - 1)}}}{\left(\frac{2}{\gamma_1 + 1} \right)^{\frac{\gamma_1 + 1}{2(\gamma_1 - 1)}}} \left[(T_d/T_t)_2 \right]^{\frac{\gamma_2 - \gamma_1}{\gamma_1(\gamma_2 - 1)}} \left[\frac{1 - (T_d/T_t)_2}{1 - (T_d/T_t)_2} \right]^{1/2} \quad (15)$$

With Eq. (15) it is possible to estimate the value of the function R_2 required if ejector configuration "2" is to simulate the performance of ejector configuration "1". To do this it is necessary to estimate the temperature ratio $(T_d/T_t)_2$ which is related to the minimum cell pressure ratio $(p_c/p_{pt})_2$. For most ejector configurations the minimum cell pressure can be roughly estimated using the data presented in this report.

If it is assumed that the function R can be represented by the right-hand side of Eq. (2) then the value of either R_1 or R_2 determined by Eq. (15) must always lie in the range 0.5 to 1.159 if the similarity rule is to be valid.

The present experimental data are too limited to verify Eq. (15).

SUMMARY OF RESULTS

The results of an investigation to determine the effects of nozzle total pressure level on ejector performance can be summarized as follows:



1. The minimum cell pressure ratio was a strong function of nozzle total pressure level when the parameter, unit Reynolds number at the nozzle exit times the nozzle throat diameter, was less than 1.0×10^6 .

2. For ejectors equipped with conical nozzles having half angles of 15 or 18 deg, the corresponding minimum cell pressure ratios can be estimated to ± 20 percent using an empirical equation.
3. The variation of minimum cell pressure ratio with nozzle total pressure level for ejectors equipped with contoured nozzles having 0-deg exit angles was similar to that exhibited by ejectors equipped with 18-deg conical nozzles.
4. The ejector operating pressure ratios, p_{ex}/p_{pt} , were essentially independent of the nozzle total pressure level.

REFERENCES

1. Barton, D. L. and Taylor, D. "An Investigation of Ejectors without Induced Flow, Phase I." AEDC-TN-59-145, December 1959.
2. Taylor, D., Barton, D. L., and Simmons, M. "An Investigation of Cylindrical Ejectors Equipped with Truncated Conical Inlets, Phase II." AEDC-TN-60-224, March 1961.
3. German, R. C. and Bauer, R. C. "The Effect of Diffuser Length on the Performance of Ejectors without Induced Flow, Phase III." AEDC-TN-61-89, August 1961.
4. Crocco, Luigi and Lees, Lester. "A Mixing Theory for the Interaction between Dissipative Flows and Nearly Isentropic Streams." Princeton University, Aeronautical Engineering Laboratory, Report No. 187, January 15, 1952.
5. Korst, H. H., Chow, W. L., and Zumwalt, G. W. "Research on Transonic and Supersonic Flow of a Real Fluid at Abrupt Increases in Cross Section (With Special Considerations of Base Drag Problems), Final Report." University of Illinois, ME-TR-392-5, December 1959.
6. Goethert, B. H. "Base Flow Characteristics of Missiles with Cluster-Rocket Exhausts." Aerospace Engineering, March 1961.
7. Mickola, Richard H. "Performance Summary of the Supersonic Diffuser and Its Application to Altitude Testing of Captive Rocket Engines." Addendum I to AFFTC-TR-60-1, April 1961.

TABLE 1
DESCRIPTION OF NOZZLES, DUCTING, AND SUBSONIC DIFFUSERS

Nozzle Dimensions					Duct Config. a		Duct Config. c	
Nozzle Config.	A_{ne}/A^*	D^* , in.	D_{ne} , in.	θ_n , deg	D_d , in.	A_d/A^*	D_d , in.	A_d/A^*
1	3.627	2.2	4.190	18	6.09	7.66	10.19	21.45
2	5.070	1.852	4.170	18		10.81		30.27
3	10.848	1.2615	4.155	18		23.30		65.25
4	25.00	0.831	4.155	18		53.70		150.36
5	23.684	0.900	4.380	0		45.79		128.19
6	100.00	0.442	4.420	0		189.8		531.40
7	10.962	2.38	7.880	19	$D_{ne} > D_d$		10.19	18.33
Deviation		± 0.001	± 0.001		± 0.01		± 0.01	

Subsonic Diffuser	L_s , in.	θ_s , deg	Inlet Diam, in.
S_1	97	4	6.09
S_2	76		10.19
S_3	16		6.09
S_4	13	4	10.19
Deviation	± 0.25		± 0.01

TABLE 2
SUMMARY OF TEST DATA *

Config.	Nozzle Plenum Total Pres- sure, p_{pt} , psia	Nozzle Plenum Total Temp, T_t , °F	Min Cell Pressure Ratio, p_c/p_{pt}	Starting Pressure Ratio, p_{ex}/p_{pt}	Nozzle Exit Static Pressure Ratio p_{ne}/p_{pt}
1as ₁	1.40	75	.0176	—	—
	1.99	↓	.0176	—	—
	2.89	↓	.0174	—	.0304
	3.85	↓	.0170	—	.0305
	4.86	↓	.0165	.165	.0308
	9.63	↓	.0133	—	.0312
	14.35	↓	.0113	—	.0310
	19.45	↓	.00957	—	.0310
	23.96	↓	.00861	—	.0309
	28.98	↓	.00836	—	.0309
	37.61	75	.00992	—	—
1cs ₂	7.08	75	.00403	.0560	—
	9.58	↓	.00363	.0583	—
	14.35	↓	.00328	.0578	—
	18.87	↓	.00288	.0577	—
	24.12	↓	.00240	.0588	—
	28.36	↓	.00236	.0589	—
	33.18	↓	.00245	.0599	—
	37.56	75	.00270	.0603	—
2as ₁	2.40	70	.0113	—	.0213
	3.33	↓	.0113	—	.0202
	4.94	↓	.0113	—	.0206
	7.15	↓	.0112	—	.0212
	10.34	↓	.0104	.125	—
	15.15	↓	.0097	.124	.0215
	19.25	↓	.00904	.127	.0217
	24.20	↓	.0079	.124	.0216
	29.7	↓	.00592	.124	.0216
	34.8	↓	.00517	.124	.0219
	35.7	70	.00523	.124	.022
2as ₃	44.16	50	.00553	.118	.0218
	64.16	↓	.00575	—	.0215
	84.16	↓	.00582	—	.0221
	104.36	↓	.00587	—	.0220
	133.66	↓	.00593	.118	.0218
	166.66	↓	.00570	—	.0219
	217.16	50	.00599	—	—

* $L_d/D_d \geq 5$

TABLE 2 (Continued)

Config.	Nozzle Plenum Total Pres- sure, p_{pt} , psia	Nozzle Plenum Total Temp, T_t , °F	Min Cell Pressure Ratio, p_c/p_{pt}	Starting Pressure Ratio, p_{ex}/p_{pt}	Nozzle Exit Static Pressure Ratio p_{ne}/p_{pt}
2cs ₂	5.35	70	.00292	.0450	—
	10.10	↓	.00290	.0451	—
	19.80		.00214	.0455	—
	29.70		.00153	.0451	—
	31.90		.00145	.0451	—
	34.80		.00139	.0451	—
	36.80		.00142	.0452	—
	40.30	↓	.00145	.0452	—
	42.6	70	.00149	.0451	—
	42.4	75	.00146	.0446	—
3as ₁	4.52	65	.00385	—	—
	5.02	↓	.00382	—	.00578
	7.54		.00385	—	.00500
	9.96		.00396	—	.00476
	15.15		.00402	.0607	.00517
	20.03		.00391	—	.00517
	22.39		.00376	.0609	.00531
	24.90		.00333	—	.00532
	29.90		.00236	—	.00543
	34.90		.00201	—	.00554
	40.30	↓	.00182	—	.00559
	43.85	65	.00174	—	.00562
3as ₃	44.16	55	.00166	.0552	.00584
	64.16	↓	.00148	.0558	.00579
	84.00		.00151	.0562	.00573
	104.16		.00156	.0561	.00567
	134.16		.00169	.0561	.00570
	167.00		.00177	.0578	.00568
	217.00		.00192	.0573	.00548
	265.60	↓	.00194	—	.00554
	316.2	55	.00170	—	.00563
3cs ₂	10.75	70	.00139	.0220	—
	20.09	↓	.000925	.0218	—
	29.55		.000695	.0217	—
	32.70		.000627	.0217	—
	35.00		.000613	.0217	—
	37.25		.000577	.0218	—
	40.85		.000550	.0218	—
	44.8	↓	.00056	.0218	—
	44.90	70	.000535	.0216	—

* $L_d/D_d \geq 5$

TABLE 2 (Continued)

Config.	Nozzle Plenum Total Pres- sure, p_{pt} , psia	Nozzle Plenum Total Temp, T_t , °F	Min Cell Pressure Ratio, p_c/p_{pt}	Starting Pressure Ratio, p_{ex}/p_{pt}	Nozzle Exit Static Pressure Ratio p_{ne}/p_{pt}
3cs ₄	44.20	70	.000543	.0192	.00905
	64.2	↓	.000491	.0196	.00779
	84.2		.000459	.0201	.00713
	114.2		.000466	.0202	.00701
	169.7		.000513	—	.00637
	219.2		.000534	—	.00620
	265.7		.000547	—	.00602
	328.2	↓	.000583	—	.00612
	388.0	70	.000563	—	.00572
4a	14.92	100	.00136	—	.00123
	15.80	↓	.00133	.0213	.00116
	20.35		.00136	—	.000808
	24.85		.00137	.0229	.000817
	29.75		.00137	—	.00101
	34.80		.00128	.0227	.000945
	39.75	↓	.00114	—	.000998
	43.00	100	.00106	.0228	.000967
	44.70	195	.00118	—	.00113
	44.70	162	.00121	—	.00110
	49.70	130	.00116	.0225	.00111
	59.90	100	.000889	—	.00109
4as ₁	12.80	70	.00136	—	.00310
	14.82	↓	.00134	.0269	.00228
	19.81		.00137	.0267	.000830
	24.90		.00136	.0269	.000893
	29.85		.00126	.0265	.000972
	34.80	↓	.00111	.0266	.000917
	45.45	70	.000936	.0264	.00104
4as ₃	43.70	60	.000974	.0241	.00114
	63.40	↓	.000854	—	.00110
	84.20		.000747	—	.00113
	92.70		.000712	.0252	.00124
	114.00		.000663	—	.00114
	153.20		.000583	.0253	.00111
	217.20		.000597	.0256	.00120
	265.20		.000613	—	.00117
	316.20	↓	.000639	—	.00127
	365.70	60	.000652	—	.00123

* $L_d/D_d \geq 5$

TABLE 2 (Continued)

Config.	Nozzle Plenum Total Pres- sure, p_{pt} , psia	Nozzle Plenum Total Temp, T_t , °F	Min Cell Pressure Ratio, p_c/p_{pt}	Starting Pressure Ratio, p_{ex}/p_{pt}	Nozzle Exit Static Pressure Ratio p_{ne}/p_{pt}
4cs ₂	44.7	70	.000273	.00952	-
	20.90	↓	.000407	.00988	.00134
	25.06	↓	.000386	.00993	.00112
	29.83	↓	.000363	.00991	.00101
	34.80	↓	.000350	.00981	.000944
	39.72	↓	.000307	.00986	.000998
	45.78	70	.000275	.00969	-
	46.61	75	.000266	.00954	-
4cs ₄	53.34	60	.000279	-	.000939
	74.34	↓	.000255	-	.000807
	75.34	↓	.000226	-	.000796
	94.84	↓	.000224	-	.000948
	159.14	↓	.000188	-	.00113
	268.64	↓	.000179	-	.00112
	318.14	60	.000185	-	.00123
5a	10.00	113	.000426	-	.00406
	10.35	361	.000393	.0233	.00374
	13.95	75	.000374	-	.00298
	15.80	75	.000392	-	.00300
	19.90	75	.000369	-	.00316
	19.90	104	.000389	.0241	.00365
	20.00	240	.000363	.0242	.00363
	24.85	75	.000374	-	.00323
	29.30	100	.000383	.0244	.00359
	29.90	191	.000372	.0244	.00353
	30.00	75	.000368	.0252	.00332
	34.80	75	.000361	-	.00331
	35.10	174	.000375	.0242	.00355
	35.30	94	.000370	.0243	.00353
	39.7	163	.000365	.0247	.00356
	40.55	92	.000358	.0246	.00355
	40.60	75	.000343	.0232	.00336
	42.55	75	.000327	.0247	.00341
	50.05	92	.000340	.0244	.00354
	50.15	147	.000347	.0246	.00353
	51.15	92	.000359	.0264	.00384
	56.00	141	.000338	.0246	.00351
5as ₁	12.02	90	.000595	-	.00370
	14.98	90	.000491	-	.00329
	19.95	90	.000339	-	.00320

* $L_d/D_d \geq 5$

TABLE 2 (Continued)

Config.	Nozzle Plenum Total Pres- sure, p_{pt} , psia	Nozzle Plenum Total Temp, T_t , °F	Min Cell Pressure Ratio, p_c/p_{pt}	Starting Pressure Ratio, p_{ex}/p_{pt}	Nozzle Exit Static Pressure Ratio p_{ne}/p_{pt}
5as ₁	25.00	90	.000317	—	.00313
	29.70	↓	.000326	—	.00316
	34.90		.000319	—	.00324
	41.90	90	.000314	.030	.00332
5as ₃	44.16	50	.000315	.0132	.00382
	64.16	↓	.000294	.0138	.00387
	83.96		.000270	.0144	.00379
	104.66		.000248	.0155	.00376
	133.86		.000225	.0157	.00379
	166.76		.000209	.0163	.00378
	216.96		.000191	.0165	.00387
	265.46		.000176	.0168	.00396
	316.26	↓	.000168	.0165	.00403
	365.96	50	.000164	—	.00404
5cs ₄	44.6	70	.0000997	.0067	.00426
	64.2	↓	.0000844	.0065	.00390
	84.5		.0000778	.0067	.00414
	113.7		.0000714	—	.00405
	166.5		.0000668	—	.00372
	217.2	↓	.0000623	—	.00378
	314.2	70	.0000579	—	.00382
6a	53.0	102	.0000948	.00624	.000905
	53.8	306	.0000863	.00638	.000892
	59.4	143	.0000879	.00636	.000863
	59.8	281	.0000712	.00637	.000754
	64.3	141	.0000872	.00634	.000872
	69.2	120	.0000894	.00636	.000825
	70.0	258	.0000760	—	.000699
	79.0	108	.0000881	.00641	.000833
	89.2	100	.0000867	.00640	.000854
	98.4	94	.0000885	.00645	.000839
	99.7	206	.0000803	.00650	—
6as ₁	25.42	65	.000840	.00771	.000692
	26.70	↓	.00054	.00734	.000659
			.000400	—	—
	27.65		.000110	.00711	.000658
	28.45	↓	.000075	.00691	.000680
	29.47	65	.000072	.00670	.000690

* $L_d/D_d \geq 5$

TABLE 2 (Concluded)

Config.	Nozzle Plenum Total Pres- sure, p_{pt} , psia	Nozzle Plenum Total Temp, T_t , °F	Min Cell Pressure Ratio, p_c/p_{pt}	Starting Pressure Ratio, p_{ex}/p_{pt}	Nozzle Exit Static Pressure Ratio p_{ne}/p_{pt}
6as ₁	34.85	65	.000061	.00573	.000638
	39.70	65	.000063	.00515	.000682
	45.20	65	.0000770	.00728	.000805
6as ₃	44.09	60	.0000746	—	.00112
	64.49	↓	.0000705	.00257	.000885
	84.59	↓	.0000720	—	.00101
	104.29	↓	.0000705	.00275	.000979
	123.39	↓	.0000721	—	.00106
	166.59	↓	.0000639	.00286	.000986
	217.09	↓	.0000606	.00295	.000980
	265.09	↓	.0000562	—	.000967
	316.09	60	.0000551	—	.000970
6cs ₄	104.46	50	.0000189	.00130	.00144
	133.16	↓	.0000150	.00128	.00124
	166.66	↓	.0000124	.00142	.00114
	227.16	↓	.0000170	.00147	.000925
	265.36	↓	.0000168	.00153	.000980
	316.36	50	.0000165	.00153	.000980
7cs ₂	6.82	123	.00538	—	—
	13.85	123	.00458	.0759	—
	18.66	125	.00348	.0748	—
	27.94	130	.00245	.0753	—
	30.07	135	.00240	—	—
	32.82	138	.00236	.0767	—
	34.33	140	.00233	.0759	—
	34.42	116	.00241	.0756	—

* $L_d/D_d \geq 5$

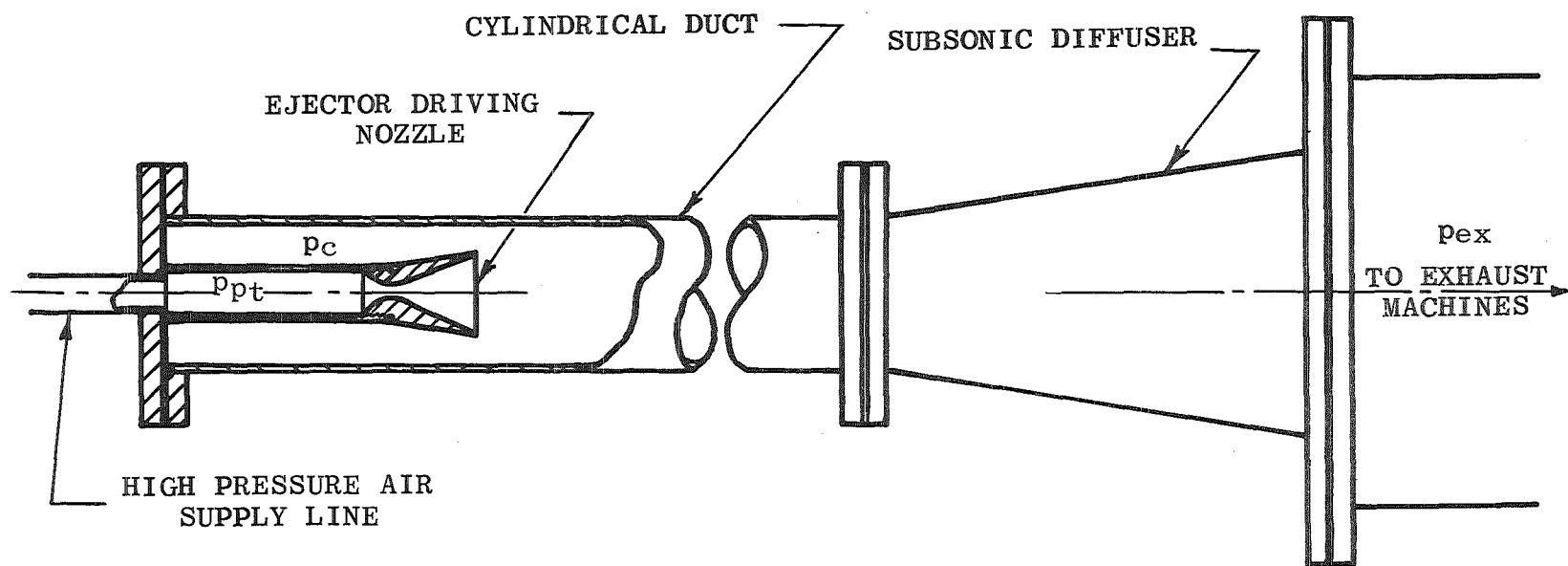
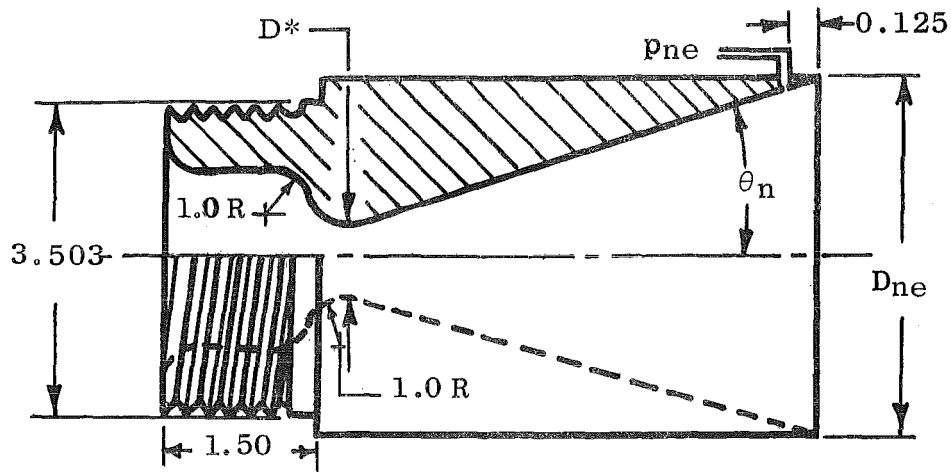
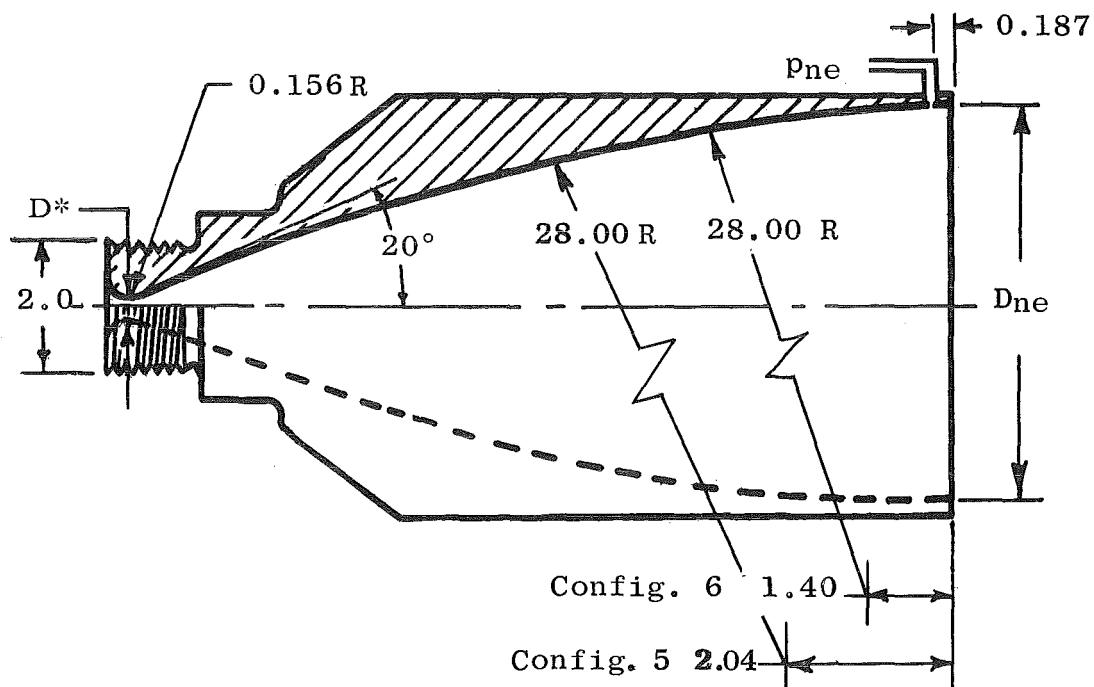


Fig. 1 Typical Ejector Configuration

All dimensions
are in inches



a. Conical Nozzle



b. Nozzle Having Zero Exit Flow Angle

Fig. 2 Typical Nozzle Configurations

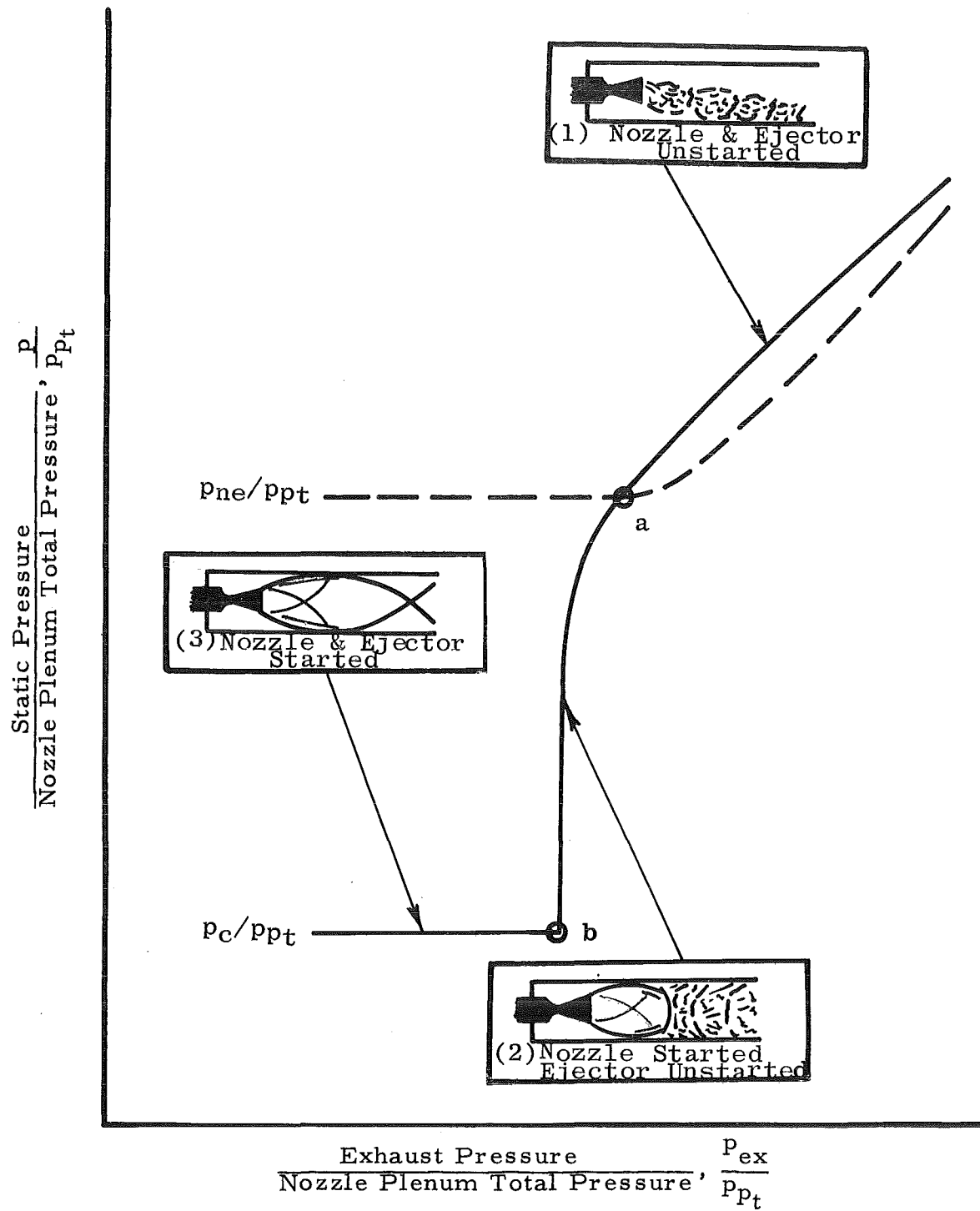


Fig. 3 Typical Ejector Starting Phenomena for Constant Nozzle Plenum Total Pressure

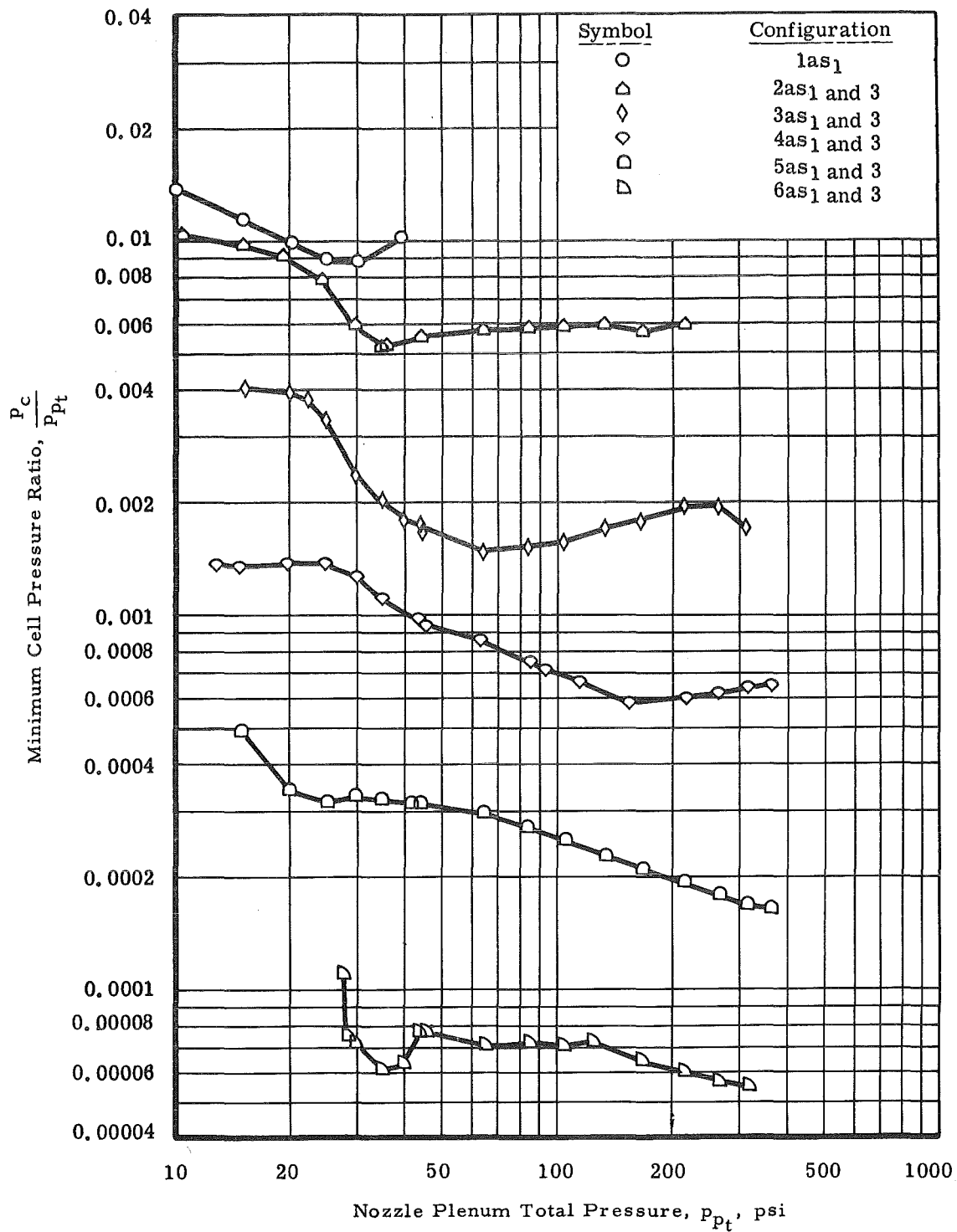


Fig. 4 Variation of Minimum Cell Pressure Ratio, p_c/p_{p_t} , with Nozzle Plenum Total Pressure Level, p_{p_t} .

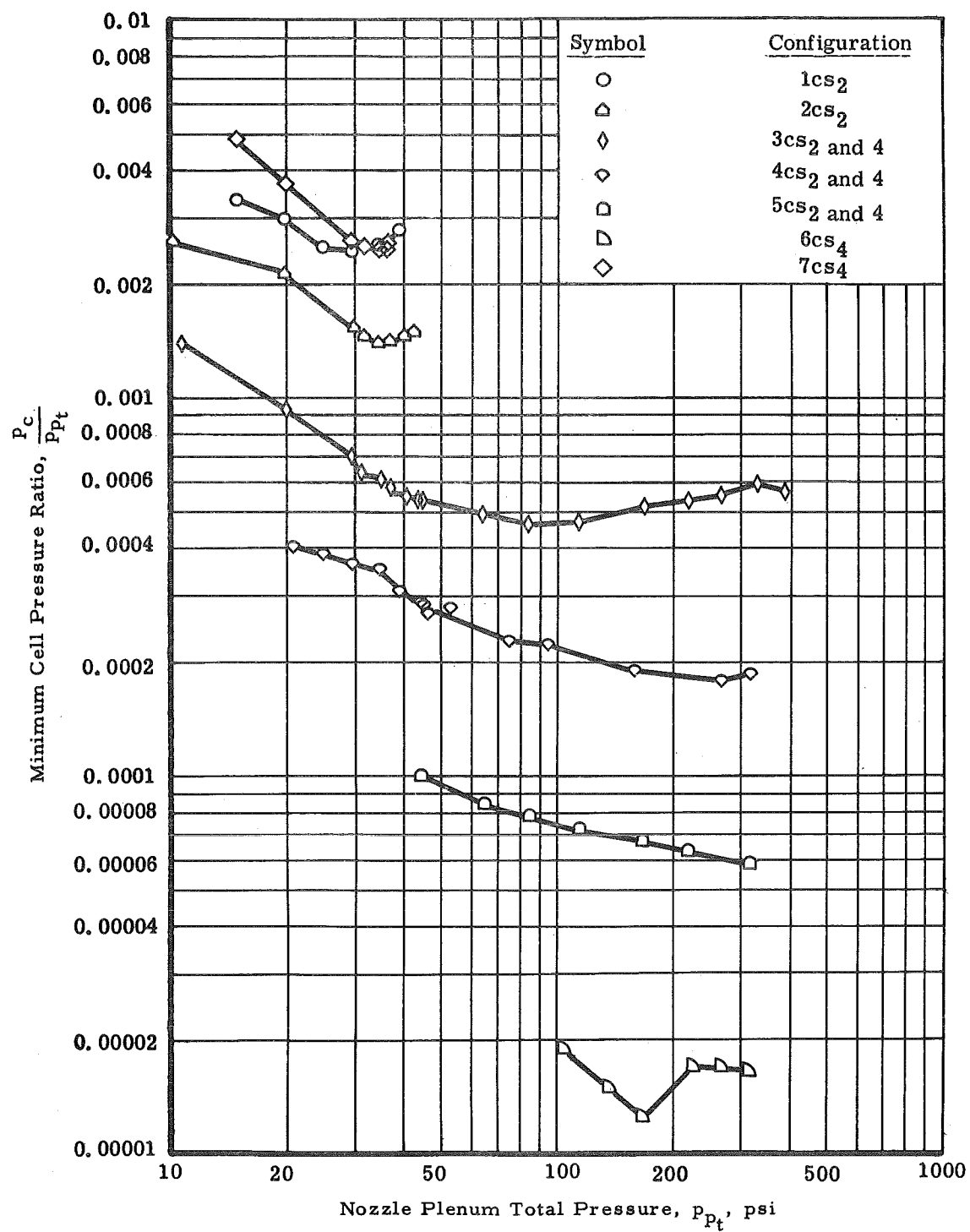
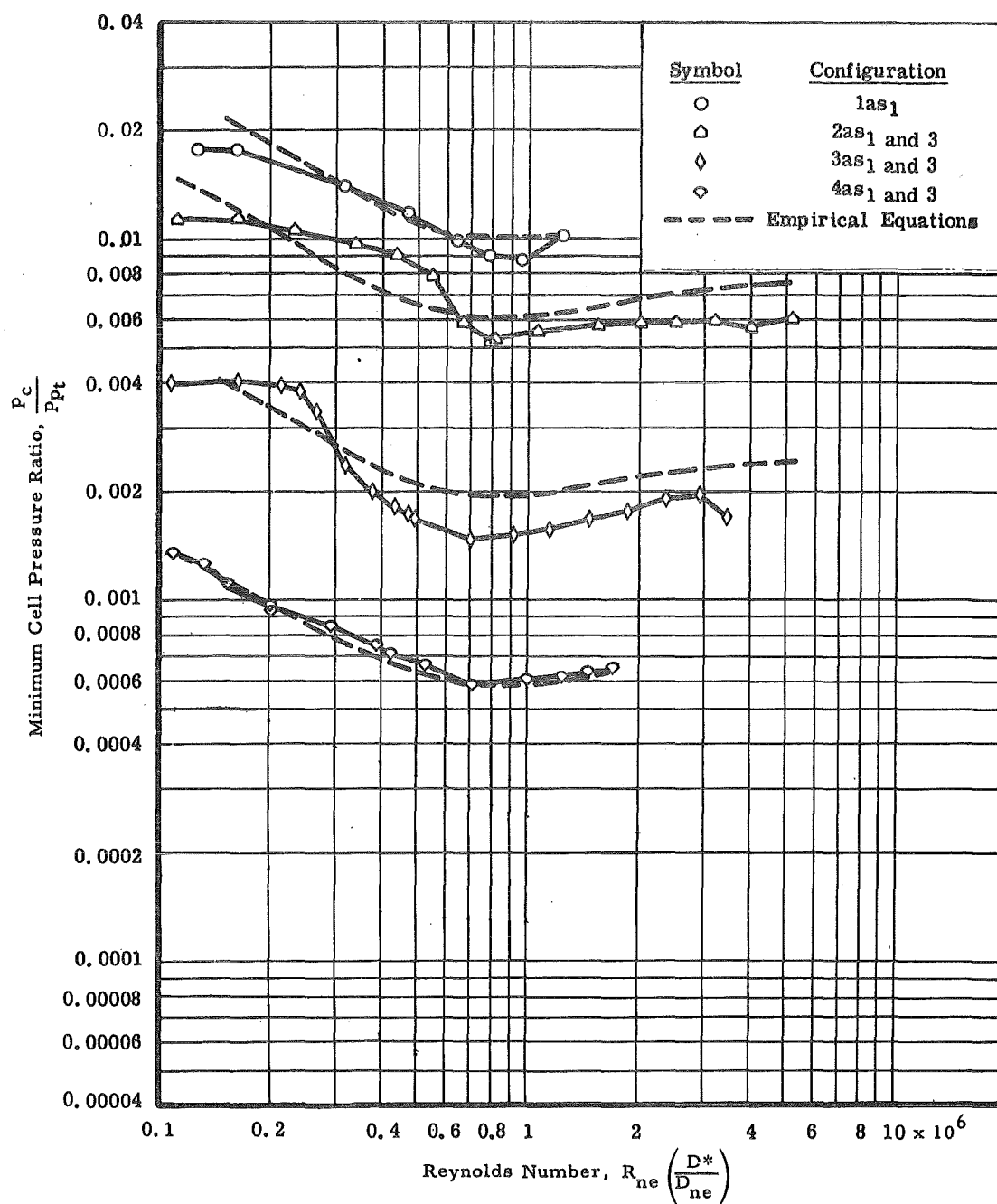
b. $D_d = 10.19$ in.

Fig. 4 Concluded



a. $D_d = 6.09$ in.

Fig. 5 Comparison of Empirical Results with Experimental Data

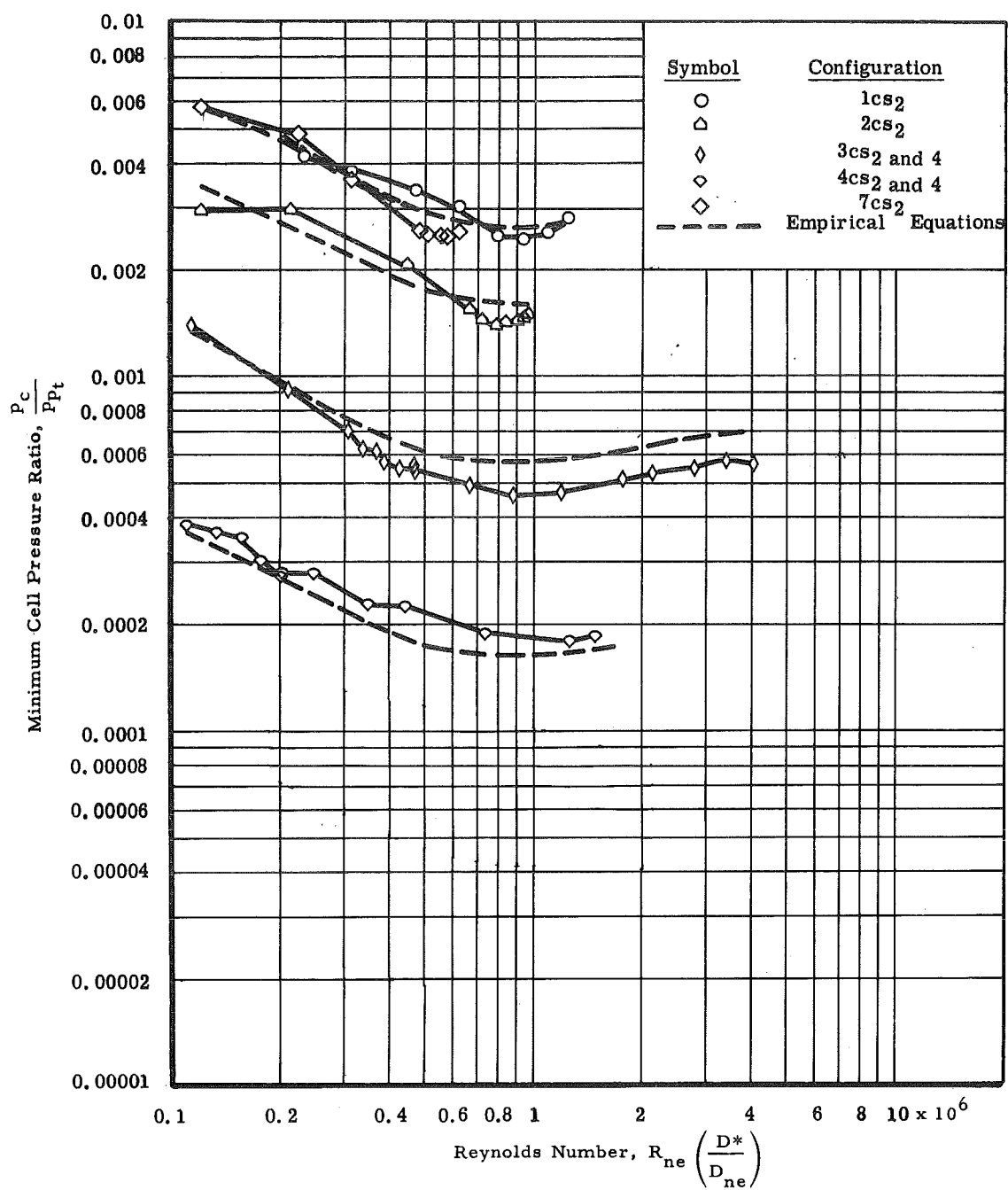
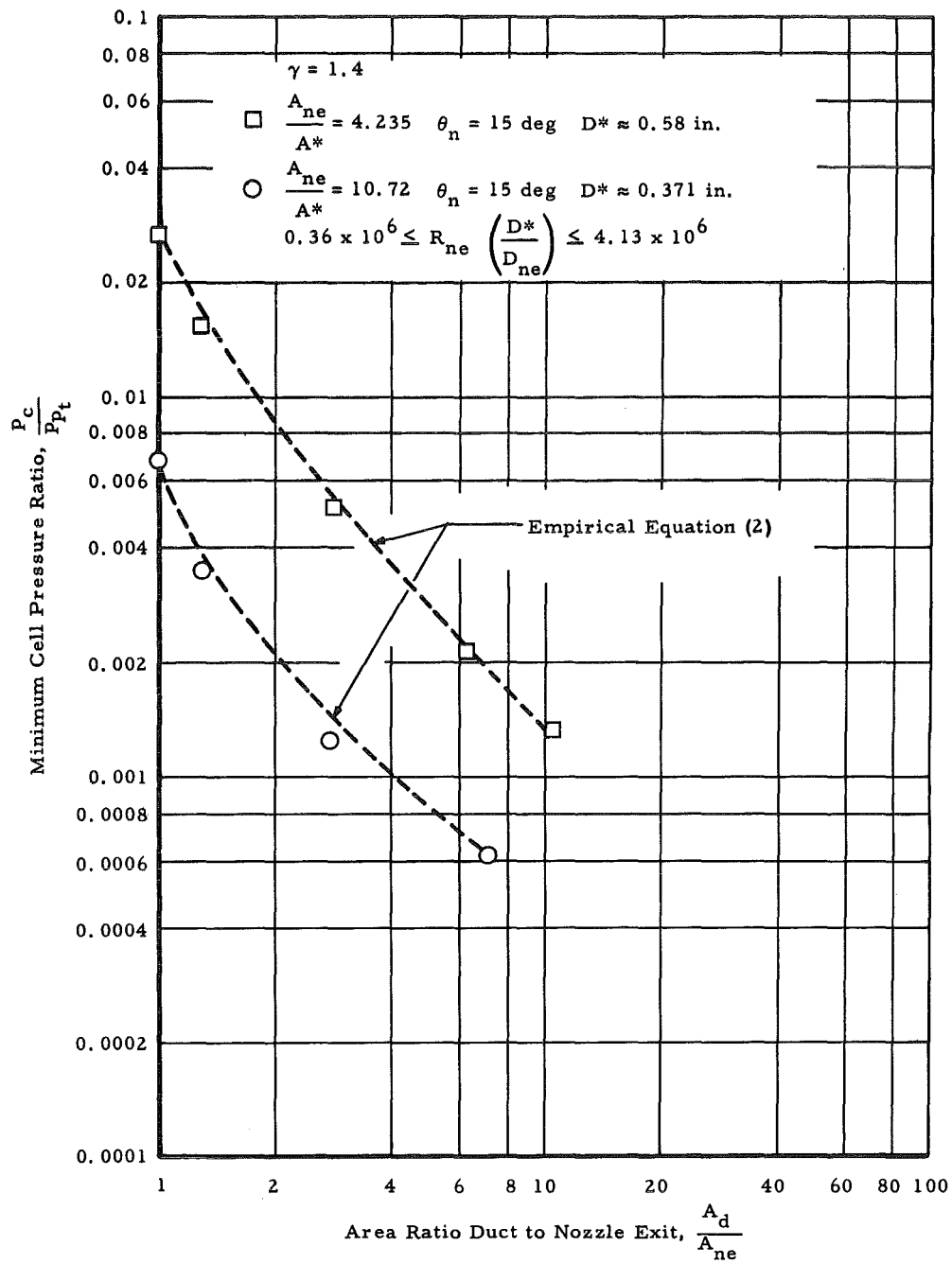
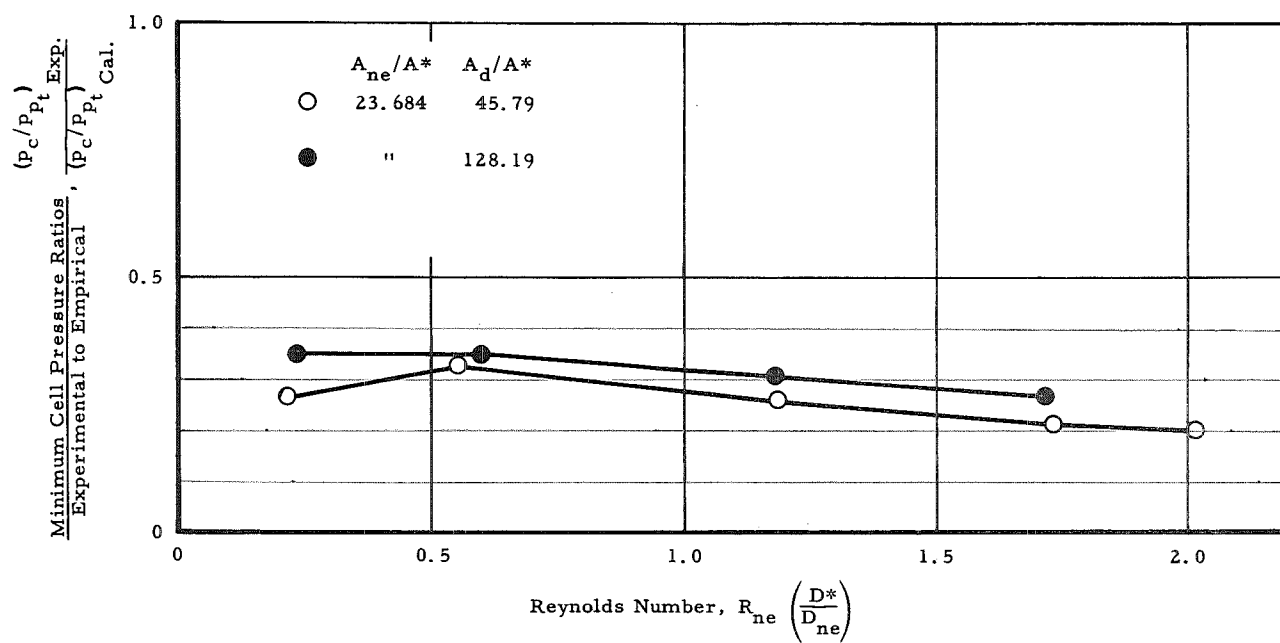
b. $D_d = 10.19$ in.

Fig. 5 Continued



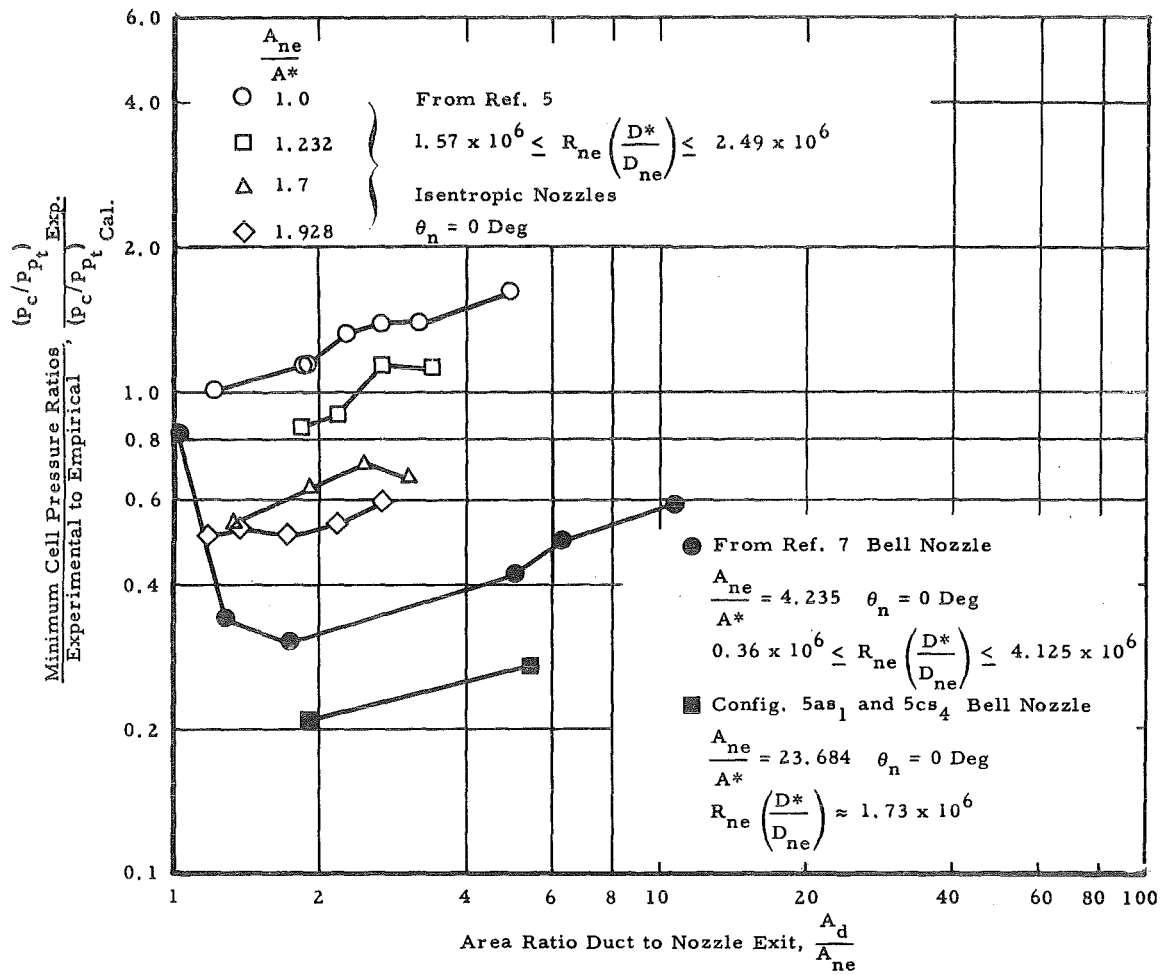
c. Data from Ref. 7

Fig. 5 Concluded



a. Data from Configs. 5as₁, 5as₃, and 5cs₄ with A_d/A^* as Parameter

Fig. 6 Comparison of Empirical Results with Experimental Data



b. Data from Refs. 5 and 7, Config. 5as₁, 5as₃, and 5cs₄ with A_{ne}/A^* as Parameter

Fig. 6 Concluded